

1 **Supporting Information**

2

3 **Reversal of air-sea exchange and accumulation of POPs (PAHs, PCBs, OCPs and**  
4 **PBDEs) in the nocturnal marine boundary layer**

5

6 Gerhard Lammel<sup>1,2\*</sup>, Franz X. Meixner<sup>3</sup>, Branislav Vrana<sup>1</sup>, Christos Efstathiou<sup>1</sup>, Jiří  
7 Kohoutek<sup>1</sup>, Petr Kukučka<sup>1</sup>, Marie D. Mulder<sup>1</sup>, Petra Přibyllová<sup>1</sup>, Roman Prokeš<sup>1</sup>, Tatsiana P.  
8 Rusina<sup>1</sup>, Guo-Zheng Song<sup>3</sup>, Manolis Tsapakis<sup>4</sup>

9

10 <sup>1</sup> Masaryk University, Research Centre for Toxic Compounds in the Environment, Brno,  
11 Czech Republic

12 <sup>2</sup> Max Planck Institute for Chemistry, Multiphase Chemistry Dept., Mainz, Germany

13 <sup>3</sup> Max Planck Institute for Chemistry, Biogeochemistry Dept., Mainz, Germany

14 <sup>4</sup> Hellenic Centre for Marine Research, Institute of Oceanography, Gournes, Greece

15

16

17 **Contents**

18 S1 Methodology

19 S1.1 Substance properties

20 S1.2 Analytical quality assurance parameters

21 S1.3 Vertical flux calculations by micrometeorological techniques

22 S1.4 Non-steady state two-box model

23 S2 Results

24 S2.1 Meteorological situation

25 S2.2 Transfer velocity

26 S2.3 Atmospheric concentration and flux data

27 S2.4 Seawater concentration data

28 S2.5 Model predicted concentrations and air-sea exchange flux

29 References

30

## 31 **S1 Methodology**

### 32 **S1.1 Substance properties**

33 For the fugacity ratio calculation based on the Whitman two-film model (Bidleman and  
34 McConnell, 1995), the Henry's law constant was corrected for the sea water temperature and  
35 the salt water (by the Setschenow constant, e.g., Zhong et al., 2012).

36

37 Table S1. References of physico-chemical properties used. H = Henry's law constant,  $dU_{aw}$  =  
38 enthalpy of water-air phase change,  $K_S$  = salting-out (Setschenow) constant. Substances  
39 addressed: see main text.

	PAHs	PCBs	OCPs	PBDEs
H	Bamford et al., 1999	Li et al., 2003	Cetin et al., 2006	Cetin and Odabasi, 2005; Tittlemier et al., 2002
$dU_{aw}$	Bamford et al., 1999	Li et al., 2003	Cetin et al., 2006	Cetin and Odabasi, 2005
$K_S$	Jonker and Muijs, 2010 <sup>(a)</sup>	Rowe et al., 2007	Lohmann et al., 2012; Cetin et al., 2006	Jonker and Muijs, 2010 <sup>(b)</sup>

40 <sup>(a)</sup> assumed to be given by value for isomer in case of lack of data

41 <sup>(b)</sup> adopted estimate

42

43

44 **S1.2 Analytical quality assurance parameters**

45 Table S2: Instrument limits of quantification (ILOQ) for various  
46 types of sample, given as masses and concentrations

Analyte	Mass	concentration	
	(pg)	air (pg m <sup>-3</sup> )	water (pg L <sup>-1</sup> )
PAHs	160-840	6-34	0.5-4.2
PCBs and OCPs	50-510	7-23	0.05 - 0.5
PBDEs	0.083-0.953	0.003-0.304	0.0003 - 0.037

47

48 **S1.3 Vertical flux calculations by micrometeorological techniques**

49 Two micrometeorological methods, the aerodynamic and the eddy covariance technique, have  
50 been applied to derive turbulent vertical gaseous organics fluxes ( $F_c$ , in ng m<sup>-2</sup> s<sup>-1</sup>). According  
51 to the aerodynamic method (Hicks et al., 1987; Kuhn et al., 2007),  $F_c$  is the product of the  
52 vertical difference of gaseous organics concentration,  $\Delta c_z$  (ng m<sup>-3</sup>), and the turbulent transfer  
53 velocity,  $v_{tr}$  (m s<sup>-1</sup>):

$$54 \quad F_c = -v_{tr} \Delta c_z = -v_{tr} [c(z_2) - c(z_1)] \quad (S1)$$

55 where  $z_2$  and  $z_1$  are the heights of inlets of gaseous organics' sampling (1.05 m and 2.80 m, see  
56 section 2.1). The transfer velocity, a measure of the vertical turbulent (eddy) diffusivity  
57 between  $z_2$  and  $z_1$ , is simply the inverse of the aerodynamic resistance,  $R_a$  (s m<sup>-1</sup>), against the  
58 vertical transport:

$$59 \quad R_a = v_{tr}^{-1} = (\kappa u_*)^{-1} [ \ln(z_{r,2}/z_{r,1}) - \Psi_H(z_{r,2}/L) + \Psi_H(z_{r,1}/L) ] \quad (S2)$$

60 where  $\kappa$  is the von Karman constant (= 0.4),  $u_*$  is the friction velocity (in m s<sup>-1</sup>),  $z_{r,i} = z_i - d$  is  
61 the relative height (in m), and  $d = 0.34$  m is the zero-plane displacement height for the Selles  
62 Beach site, derived by the eddy covariance technique. Applying the Monin-Obukhov similari-  
63 ty theory (Monin and Obukhov, 1954) for the mathematical description of turbulent transport  
64 in the atmospheric surface layer, a characteristic length scale, the Obukhov length  $L$  (in m;  
65 Obukhov, 1948) is the quantitative measure of the relation between dynamic (friction) and  
66 thermal (buoyancy) forces which drive the turbulent transport,

$$L = - u_*^3 [ \kappa g T_{\text{air}}^{-1} H (c_p \rho_{\text{air}})^{-1} ]^{-1} \quad (\text{S3})$$

68 where  $T_{\text{air}}$  is the air temperature (K),  $c_p$  is the specific heat of air at constant pressure (1004.7  
69  $\text{m}^2 \text{s}^{-2} \text{K}^{-1}$ ),  $g$  the acceleration of gravity ( $9.807 \text{ m s}^{-2}$ ), and  $H$  the turbulent sensitive heat flux  
70 ( $\text{W m}^{-2}$ ). When applying the eddy covariance technique, the key micrometeorological  
71 quantities  $u_*$  and  $H$  were derived from fast response (20 Hz) measurements of the three spatial  
72 components of the 3D wind vector and the air temperature. For control of the atmospheric sur-  
73 face layer's thermodynamic stratification vertical gradients of wind speed ( $u$ ) and air  
74 temperature ( $T_{\text{air}}$ ) have been used which in turn have been derived from continuous mea-  
75 surements of wind speed and air temperature at four levels (0.34, 0.70, 1.45, and 3.00 m above  
76 ground) at Selles Beach. The dimensionless integrated similarity functions (or integrated  
77 stability correction functions)  $\Psi_{\text{H}}(z_r, 2/L)$  and  $\Psi_{\text{H}}(z_r, 1/L)$  for heat were calculated after Paulson  
78 (1970).

79

#### 80 **S1.4 Non-steady state two-box model**

81 A non-steady state 2-box model was applied to test the hypothesis that the diurnal variation of  
82 POP concentrations in air during 6-10 July is explained by local processes, namely the  
83 combination of volatilisation from the sea surface and atmospheric mixing depth.

84 The model simulations for the period 6-10 July 2012 were initialised by observed surface  
85 seawater concentrations,  $c_w$  (Table 2), and modelled marine boundary layer depths  
86 (Lagrangian dispersion model; see Section 2.2). Temperature and wind speed data were taken  
87 from measurements at the site (Cretan north coast). Winds were on-shore throughout the  
88 simulated period. Input data are listed in Table S3. Gaseous air and seawater concentrations  
89 and the air-sea exchange flux,  $F_{\text{aw}}$ , are output.

90 Substances for which input data were incomplete or insufficient observational data were  
91 available (model evaluation) were not simulated. Upon input, simultaneous measurements of  
92 air and seawater concentrations are lacking for HCH and 3-ring PAHs (see Section 2.5) and  
93 some physic-chemical properties are lacking for PeCB. Insufficient air concentration and flux  
94 measurements during 6-10 July are available for DDE. Input parameters for the 2-box model  
95 are listed in Table S3. The biogeochemical parameters had been used earlier to simulate the  
96 air-sea exchange of a PAH in the same region (Mulder et al., 2014).

97

98 Table S3. Input parameters for the 2-box model, (a.) environmental, (b.) substance specific.

99 a.

Parameter	Unit	Value adopted or mean (min-max)	Reference
OH concentration in air	molec cm <sup>-3</sup>	1.5×10 <sup>6</sup> during day-time, 0 during nighttime	climatological data (Spivakovsky et al., 2000)
Dissolved organic carbon concentration in seawater	μM	61.5	Pujo-Pay et al., 2011
Atmospheric mixing height	m	522 (131-1295)	Modelled (see section 2.2, Fig. S1)
Mixing depth in ocean	m	40	d'Ortenzio et al., 2005
Concentration of particulate organic carbon in surface seawater	μM	3.08	Pujo-Pay et al., 2011
Air temperature	K	302.1 (299.1 – 305.1)	Measured
Surface seawater temperature (SST)	K	297.4 (297.0 – 297.9)	satellite-retrieved data <sup>a</sup>
Export (settling) velocity of particle-sorbed molecule in seawater	m s <sup>-1</sup>	8×10 <sup>-7</sup>	Schwarzenbach et al., 2003, divided by a factor of 10 (Mulder et al., 2014, upper estimate parameter set)
Deposition velocity of particle-sorbed molecule in air	m s <sup>-1</sup>	6.5×10 <sup>-5</sup>	Franklin et al., 2000

100 <sup>a</sup> AVHRR (Advanced Very High Resolution Radiometer), 1.5 × 1.5 km resolution; source: eoweb.dlr.de:8080

101

102 b.

Parameter	Unit	Value adopted or mean (min-max)	Reference
Henry coefficient	Pa m <sup>-3</sup> mol <sup>-1</sup>	FLT/PYR: 1.96/1.71 PCB28/PCB52: 18.1/14.8 PBDE47/PBDE99: 0.85/0.60	Bamford et al., 1999; Li et al., 2003; Cetin and Odabasi, 2005
1 <sup>st</sup> order degradation rate coefficient in seawater	10 <sup>-9</sup> s <sup>-1</sup>	FLT/PYR: 4.2/2.8 PCB28/PCB52: 2.2/1.2 PBDE47/PBDE99: 0/0	Value for freshwater (USEPA, 2009) divided by 10; Value for water (Beyer et al., 2000; Wania and Daly, 2002) divided by 10; T dependence: EU, 1996; assumed to be 0 in lack of data
Gas-phase reaction rate coefficient with OH	10 <sup>-12</sup> cm <sup>3</sup> molec <sup>-1</sup> s <sup>-1</sup>	FLT/PYR: 11/50 PCB28/PCB52: 0.934/0.0162 PBDE47/PBDE99: 1.5/0.80	Keyte et al., 2013; Anderson and Hites, 1996; USEPA, 2009; Raff and Hites, 2007
Octanol/water partitioning coefficient K <sub>ow</sub>	log	FLT/PYR: 5.16/4.88 PCB28/PCB52: 5.66/5.91 PBDE47/PBDE99: 6.11/6.61	Calvert et al., 2002; Li et al., 2003; Hayward et al., 2006
Dissolved organic carbon/water partition coefficient	L g <sup>-1</sup>	0.411 × K <sub>ow</sub>	Karickhoff, 1981
Particulate organic carbon/water partitioning coefficient	L g <sup>-1</sup>	K <sub>ow</sub>	assumed to be given by K <sub>ow</sub> (Rowe et al., 2009)
Setschenow constant	L mol <sup>-1</sup>	FLT/PYR: 0.364/0.354 PCB28/PCB52: 0.3/0.3 PBDE47/PBDE99: 0.35/0.35	Jonker and Muijs, 2010; Cetin et al., 2006; Rowe et al., 2007; Jonker and Muijs, 2010
Particulate mass fraction in air		0.05 (0.02 - 0.14)	Measured

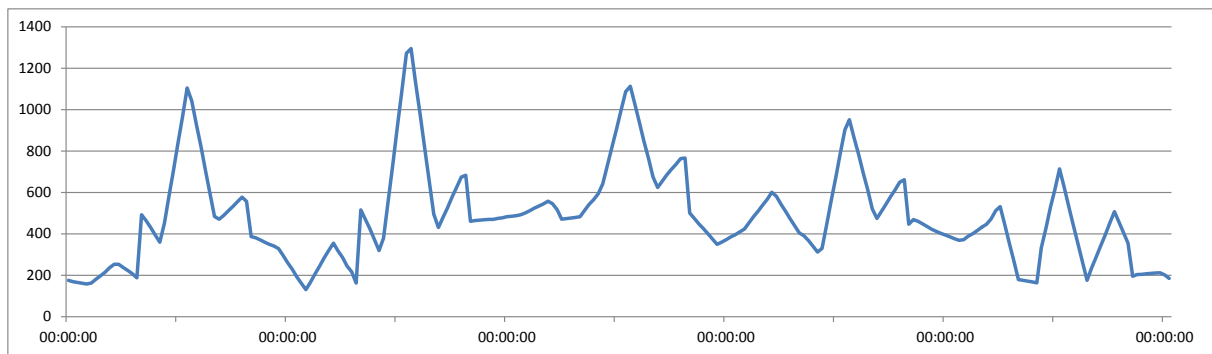
103

104 Table S4. Measured sea surface temperature 6-10 July 2012 (°C), AVHRR, 12 h means,  
105 resolution 1.5 × 1.5 km (Valavanis et al., 2004), input for simulation of c<sub>a</sub>

Date	Day	Night
20120706	24.749	23.837
20120707	24.202	23.972
20120708	24.626	24.536
20120709	24.115	24.297
20120710	23.91	23.914

106

107 Fig. S.1. Modelled atmospheric mixing depth (m) 6-10 July 2012 (UTC), input for simulation  
108 of c<sub>a</sub>



109

110

## 111 **S2 Results**

### 112 **S2.1 Meteorological situation**

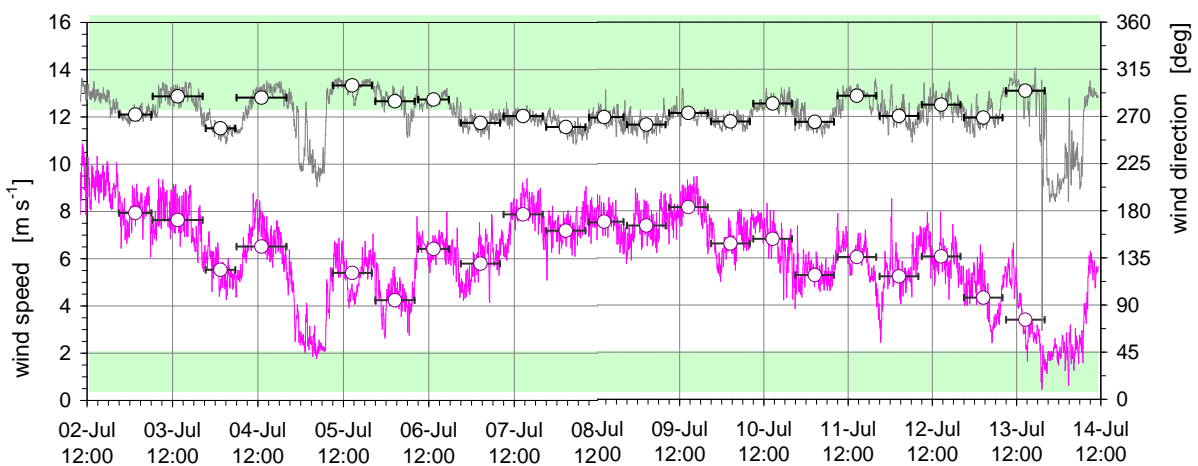
113 During 2-11 July 2012 the Aegean was mostly influenced by northerly, and in its northern part  
 114 easterly advection over the Marmara Sea as part of a cyclonic system which resided over  
 115 Romania during 1-3 July and over western Russia during 4-10 July. The sky was cloud-free all  
 116 the time. No frontal passage occurred, such that for all samples taken in the study region the  
 117 hypothesis of horizontal homogeneity of air mass collected can be applied. Under the  
 118 influence of a strong westerly flow towards Europe the flow in the northern part of the Aegean  
 119 switched to westerly during the night 11-12 July, such that air which was residing over the  
 120 SW Balkans was advected as well as air from beyond, i.e. central Italy and the NW  
 121 Mediterranean Sea and the Iberian Peninsula.

122 The local meteorological situation for the entire sampling campaign (2–13 July 2012) is given  
 123 in Fig. S2, showing the temporal course of wind speed and direction measured at the position  
 124 of one of the automatic weather stations at Selles Beach. Surprisingly, >80% of the campaign  
 125 (and >95% of the gradient measurements i.e., horizontal bars in Fig. S2) experienced wind  
 126 speeds  $> 4 \text{ m s}^{-1}$ . Under such conditions a local wind system (land-sea breeze) is most  
 127 unlikely. Consequently, as soon as the wind speed broke down to  $< 3 \text{ m s}^{-1}$ , land-sea breeze  
 128 occurred (nights 5-6 July, 13-14 July, Fig. S2) Under these conditions the atmospheric  
 129 surface layer is usually very well mixed due to the dynamic forces (friction), such that thermal  
 130 stability corrections in eq. (S2) can be neglected ( $\Psi_H(z_r,2/L) = \Psi_H(z_r,1/L) \approx 0$ ).

131 The local wind direction, however, was almost thoroughly from the west ( $270^\circ$ ), within a  
132 quite narrow range ( $259^\circ$ – $300^\circ$ ; averages during individual sampling periods given in  
133 Fig. S2). Only winds between  $270^\circ$  and  $40^\circ$  (condition for onshore winds) could be considered  
134 for the evaluation of turbulent vertical fluxes,  $F_c$ , from and to seawater. All individual  
135 sampling periods with more than 10% of the time outside this wind sector were rejected  
136 (nights 3-4 July, 4-5 July, 6-7 July, 7-8 July, 8-9 July, 9-10 July, 10-11 July).

137

138 Fig. S2: Wind speed (magenta) and wind direction (grey) observed on Selles Beach during 2-  
139 14 July 2012. White circles represent central values of sampling intervals. Horizontal bars  
140 indicate the length of intervals. Green shaded area = on-shore winds. For flux calculations  
141 only intervals with on-shore wind were used.



142

143

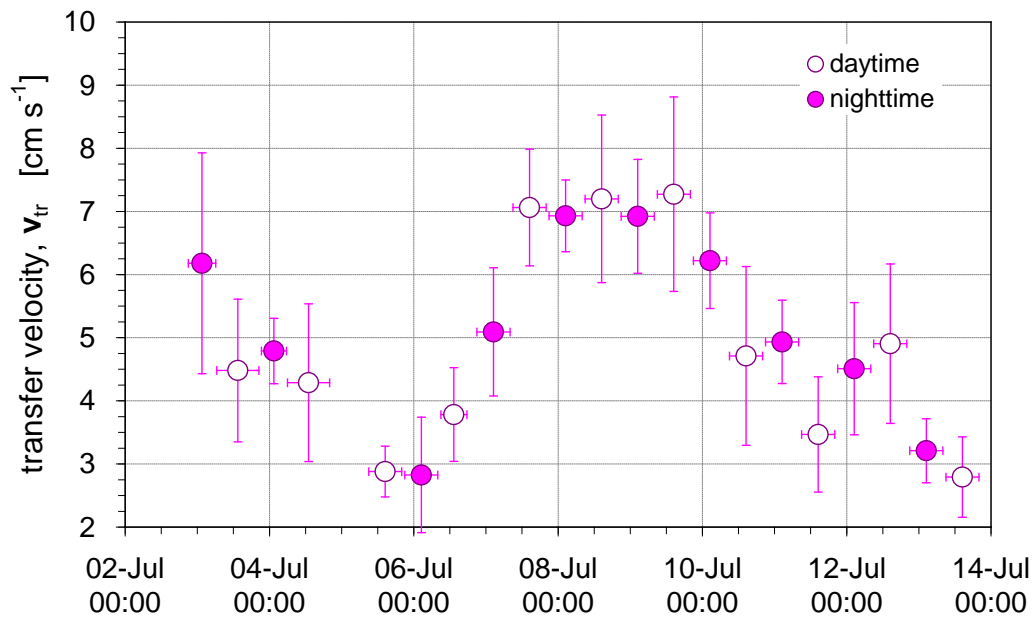
## 144 S2.2 Transfer velocity

145 The time series of turbulent transfer velocity,  $v_{tr}$ , at Selles Beach, derived from micrometeorological  
146 measurements by eddy covariance technique (sections 2.4, S1.3), is shown in Fig. S3.  
147 Data represent temporal averages of 30 min  $v_{tr}$  values over each individual sampling period  
148 (mostly 11 h), horizontal bars indicate the length of the sampling period, and vertical error  
149 bars correspond to  $\pm 1\sigma$  of the respective  $v_{tr}$  mean. Since only those data from periods with  
150 winds from the sea (onshore winds between  $270^\circ$  and  $40^\circ$ ) could be considered for suitable  
151 fetch conditions, data of the nights 3-4 July and in the period 6-11 July have not been used for  
152 calculations of vertical fluxes. Values of transfer velocity range between approx. 2.5 and 7.5

153  $\text{cm s}^{-1}$ , and – since turbulent transport at Selles Beach was dominated by dynamic forces,  $v_{tr}$   
154 data mirror more or less those of horizontal wind speed (see Fig. S2).

155

156 Fig. S3: Turbulent transfer velocities ( $\text{cm s}^{-1}$ ) during the field campaign at Selles Beach, Crete  
157 ( $35.2^\circ\text{N}$ ,  $24.4^\circ\text{E}$ ) during 2-13 July 2012. Eddy covariance technique and calculations have  
158 been applied to derive these data from measurements of fast response (20 Hz) measurements  
159 of key micrometeorological parameters (details, see S1.3).



160

161

162 **S2.3 Atmospheric concentration and flux data**

163 Table S3. Concentrations at ground level,  $z_1 = 1.05$  m, of (a.) gaseous and particulate PAHs  
 164 ( $\text{ng m}^{-3}$ ), and (b.) gaseous OCPs ( $\text{ng m}^{-3}$ ), PCBs ( $\text{ng m}^{-3}$ ) and gaseous and particulate PBDEs  
 165 ( $\text{pg m}^{-3}$ ) from 3 July 2012 day-time (D) until 13 July 2012 day-time. N = night-time. Upper  
 166 limits: Insignificant data ( $<3$  standard deviations of field blank concentrations). Data from 6  
 167 July D until 10 July D based on 2 replica measurements (mean).

168 a.

	ACE		PHE		FLT		PYR	
	g	p	g	p	g	p	g	p
3 July D	<0.058	<0.004	2.933	0.159	0.893	0.117	0.367	<0.003
3-4 July N	<0.096	<0.004	1.058	0.294	0.759	0.198	0.344	<0.003
4 July D	<0.058	<0.004	3.543	0.158	0.782	0.162	0.858	<0.003
4-5 July N	n.d.	n.d.	n.d.	n.d.	n.d.	n.d.	n.d.	n.d.
5 July D	<0.072	<0.004	2.366	0.126	0.634	<0.019	0.237	<0.003
5-6 July N	0.274	n.d.	4.507	n.d.	0.828	n.d.	0.930	n.d.
6 July D	0.068	<0.004	1.363	0.672	0.549	0.354	0.276	0.111
6-7 July N	0.119	<0.004	1.375	0.374	0.301	0.208	0.152	0.064
7 July D	0.081	<0.004	1.047	0.290	0.248	0.152	0.140	0.056
7-8 July N	0.116	<0.004	1.339	0.309	0.265	0.159	0.149	0.065
8 July D	0.091	<0.004	1.693	0.260	0.261	0.152	0.145	0.056
8-9 July N	0.107	<0.004	2.339	0.234	0.271	0.134	0.132	<0.003
9 July D	0.081	n.d.	0.591	n.d.	0.239	n.d.	0.090	n.d.
9-10 July N	0.110	<0.004	1.864	0.266	0.289	0.144	0.136	0.060
10 July D	0.059	<0.004	1.256	0.200	0.263	0.124	0.130	<0.003
10-11 July N	0.083	n.d.	0.756	n.d.	0.264	n.d.	0.133	n.d.
11 July D	n.d.	n.d.	n.d.	n.d.	n.d.	n.d.	n.d.	n.d.
11-12 July N	<0.072	<0.004	0.308	<0.065	0.046	<0.019	<0.10	<0.003
12 July D	<0.072	<0.004	0.246	<0.065	0.044	<0.019	<0.10	<0.003
12-13 July N	<0.072	<0.004	0.215	<0.065	0.059	<0.019	<0.10	<0.003
13 July D	<0.072	<0.004	0.567	<0.065	0.092	<0.019	<0.10	<0.003

169

	$\alpha$ -HCH	$\gamma$ -HCH	PCB28	PCB52	PCB101	<i>p,p'</i> -DDE	PBDE47		PBDE99	
	g	g	g	g	g	g	g	p	g	p
3 July D	0.078	0.242	0.037	0.023	0.008	0.015	<0.38	n.d.	<0.30	n.d.
3-4 July N	0.055	0.194	0.024	0.016	0.009	0.012	<0.38	n.d.	<0.30	n.d.
4 July D	0.008	0.007	0.006	0.003	0.005	0.003	<0.38	n.d.	<0.30	n.d.
4-5 July N	n.d.	n.d.	n.d.	n.d.	n.d.	n.d.	n.d.	n.d.	n.d.	n.d.
5 July D	0.028	0.105	0.015	0.009	0.006	0.006	<0.38	n.d.	<0.30	n.d.
5-6 July N	n.d.	n.d.	n.d.	n.d.	n.d.	n.d.	n.d.	n.d.	n.d.	n.d.
6 July D	0.017	0.042	0.021	0.010	<0.012	<0.008	0.500	0.161	0.313	0.203
6-7 July N	0.053	0.123	0.021	0.012	0.003	<0.008	<0.38	0.110	0.214	0.166
7 July D	0.029	0.065	0.022	0.010	<0.012	<0.008	0.509	0.104	0.299	0.145
7-8 July N	0.039	0.115	0.023	0.014	0.006	0.006	0.317	0-108	0.161	0.140
8 July D	0.024	0.074	0.020	0.010	<0.012	<0.008	0.345	0.132	0.264	0.192
8-9 July N	0.055	0.189	0.032	0.024	0.011	0.007	0.251	0.113	0.209	0.174
9 July D	0.019	0.046	0.024	0.010	<0.012	0.005	0.203	0.114	0.137	0.147
9-10 July N	0.076	0.245	0.033	0.024	0.011	0.007	0.228	0.135	0.197	0.152
10 July D	0.042	0.154	0.022	0.014	0.005	0.004	<0.38	0.134	<0.30	0.159
10-11 July N	0.014	0.066	<0.015	0.005	<0.012	<0.008	<0.38	0.110	0.141	0.137
11 July D	0.027	0.066	0.030	0.013	<0.008	0.010	0.262	0.105	<0.30	0.134
11-12 July N	<0.015	0.057	0.008	0.005	<0.012	<0.008	<0.38	n.d.	0.249	n.d.

12 July D	<0.015	0.038	0.008	0.003	<0.012	<0.008	<0.38	n.d.	<0.30	n.d.
12-13 July N	<0.015	0.030	0.008	0.003	<0.012	<0.008	<0.38	n.d.	<0.30	n.d.
13 July D	0.042	0.145	0.016	0.013	<0.012	0.004	<0.38	n.d.	<0.30	n.d.

171

172

173 Table S4. Vertical concentration differences,  $\Delta c_z = c_{z2} - c_{z1}$ , of gaseous (a.) gaseous and particulate PAHs ( $\text{ng m}^{-3}$ ), and (b.) gaseous OCPs ( $\text{ng m}^{-3}$ ),  
 174 PCBs ( $\text{ng m}^{-3}$ ) and gaseous and particulate PBDEs ( $\text{pg m}^{-3}$ ).  $\Delta z = 1.75 \text{ m}$ . Upper limits: Insignificant values of concentration differences ( $<6$   
 175 standard deviations of field blank concentrations).  $c_{z1}$  data from 6 July D until 10 July D based on 2 replica measurements (mean).

176 a.

	ACE		PHE		FLT		PYR	
	g	p	g	p	g	p	g	P
3 July D	<0.058	<0.007	7.35	< $\pm$ 0.129	-0.46	< $\pm$ 0.037	-0.15	n.d.
3-4 July N	<0.096	<0.007	5.55	< $\pm$ 0.129	-0.25	0.047	0.11	n.d.
4 July D	<0.058	<0.007	0.65	< $\pm$ 0.129	-0.24	< $\pm$ 0.037	-0.42	n.d.
4-5 July N	n.d.	n.d.	n.d.	n.d.	n.d.	n.d.	n.d.	n.d.
5 July D	<0.072	<0.007	0.53	< $\pm$ 0.129	-0.39	0.048	-0.13	n.d.
5-6 July N	n.d.	n.d.	n.d.	n.d.	n.d.	n.d.	n.d.	n.d.
6 July D	0.10	< $\pm$ 0.007	1.48	-0.248	< $\pm$ 0.076	-0.111	< $\pm$ 0.076	-0.041
6-7 July N	-0.024	< $\pm$ 0.007	< $\pm$ 0.37	< $\pm$ 0.129	0.18	< $\pm$ 0.037	< $\pm$ 0.076	-0.006
7 July D	-0.026	< $\pm$ 0.007	< $\pm$ 0.37	< $\pm$ 0.129	< $\pm$ 0.076	< $\pm$ 0.037	< $\pm$ 0.076	< $\pm$ 0.005
7-8 July N	< $\pm$ 0.013	< $\pm$ 0.007	0.62	< $\pm$ 0.129	0.37	< $\pm$ 0.037	0.14	< $\pm$ 0.005
8 July D	-0.019	< $\pm$ 0.007	0.76	< $\pm$ 0.129	0.41	< $\pm$ 0.037	0.16	< $\pm$ 0.005
8-9 July N	< $\pm$ 0.013	< $\pm$ 0.007	0.97	< $\pm$ 0.129	0.89	< $\pm$ 0.037	0.40	0.056
9 July D	n.d.	n.d.	n.d.	n.d.	n.d.	n.d.	n.d.	n.d.
9-10 July N	0.037	< $\pm$ 0.007	0.80	< $\pm$ 0.129	0.95	< $\pm$ 0.037	0.45	< $\pm$ 0.005
10 July D	n.d.	< $\pm$ 0.007	0.51	< $\pm$ 0.129	0.73	< $\pm$ 0.037	0.32	0.059
10-11 July N	n.d.	n.d.	n.d.	n.d.	n.d.	n.d.	n.d.	n.d.
11 July D	n.d.	n.d.	< $\pm$ 0.37	n.d.	0.15	n.d.	< $\pm$ 0.075	n.d.
11-12 July N	n.d.	n.d.	< $\pm$ 0.37	n.d.	0.12	n.d.	< $\pm$ 0.075	n.d.
12 July D	n.d.	n.d.	< $\pm$ 0.37	n.d.	< $\pm$ 0.076	n.d.	< $\pm$ 0.075	n.d.
12-13 July N	n.d.	n.d.	< $\pm$ 0.37	n.d.	0.44	n.d.	0.18	n.d.
13 July D	n.d.	n.d.	7.35	n.d.	-0.46	n.d.	-0.15	n.d.

177

	$\alpha$ -HCH	$\gamma$ -HCH	PCB28	PCB52	PCB101	<i>p,p'</i> -DDE	PBDE47		PBDE99	
	g	g	g	g	g	g	g	p	g	p
3 July D	0.675	0.890	0.155	0.120	0.044	<±0.008	n.d.	n.d.	n.d.	n.d.
3-4 July N	0.258	0.510	0.103	0.089	0.035	<±0.008	n.d.	n.d.	n.d.	n.d.
4 July D	0.187	0.483	0.080	0.052	0.016	<±0.008	n.d.	n.d.	n.d.	n.d.
4-5 July N	n.d.	n.d.	n.d.	n.d.	n.d.	n.d.	n.d.	n.d.	n.d.	n.d.
5 July D	0.147	0.313	0.060	0.035	0.011	<±0.008	n.d.	n.d.	n.d.	n.d.
5-6 July N	n.d.	n.d.	n.d.	n.d.	n.d.	n.d.	n.d.	n.d.	n.d.	n.d.
6 July D	0.078	0.189	0.029	0.012	n.d.	n.d.	-0.28	<±0.076	<±0.33	<±0.099
6-7 July N	-0.036	-0.057	<±0.016	<±0.007	n.d.	n.d.	n.d.	<±0.076	n.d.	<±0.099
7 July D	<±0.020	-0.041	<±0.016	<±0.007	n.d.	n.d.	n.d.	<±0.076	n.d.	<±0.099
7-8 July N	-0.025	-0.048	<±0.016	<±0.007	<±0.008	<±0.008	n.d.	<±0.076	n.d.	<±0.099
8 July D	<±0.020	-0.018	<±0.016	<±0.007	n.d.	n.d.	<±0.24	<±0.076	<±0.33	<±0.099
8-9 July N	-0.025	-0.082	<±0.016	-0.0089	<±0.008	<±0.008	n.d.	<±0.076	<±0.33	<±0.099
9 July D	<±0.020	0.037	<±0.016	<±0.007	n.d.	n.d.	n.d.	-0.114	n.d.	-0.147
9-10 July N	-0.048	-0.159	<±0.016	-0.011	<±0.008	<±0.008	n.d.	<±0.076	n.d.	<±0.099
10 July D	<±0.020	-0.052	<±0.016	<±0.007	<±0.008	0.0091	n.d.	<±0.076	n.d.	<±0.099
10-11 July N	n.d.	n.d.	n.d.	n.d.	n.d.	n.d.	n.d.	n.d.	n.d.	n.d.
11 July D	<±0.020	0.088	<±0.016	<±0.007	n.d.	<±0.008	n.d.	-0.105	n.d.	-0.134
11-12 July N	n.d.	-0.030	<±0.016	<±0.007	n.d.	n.d.	n.d.	n.d.	n.d.	n.d.
12 July D	n.d.	<±0.019	<±0.016	<±0.007	n.d.	n.d.	n.d.	n.d.	n.d.	n.d.
12-13 July N	n.d.	<±0.019	<±0.016	<±0.007	n.d.	n.d.	n.d.	n.d.	n.d.	n.d.
13 July D	<±0.020	-0.073	0.017	<±0.007	n.d.	<±0.008	n.d.	n.d.	n.d.	n.d.

181 Table S5. Vertical fluxes  $F_c = -v_{tr} \Delta c_z$  of gaseous (a.) PAHs ( $\mu\text{g m}^{-2} \text{d}^{-1}$ ), and (b.) OCPs ( $\mu\text{g m}^{-2} \text{d}^{-1}$ ), PCBs ( $\mu\text{g m}^{-2} \text{d}^{-1}$ ) and PBDEs ( $\text{ng m}^{-2} \text{d}^{-1}$ ).  
 182 Positive = upward, negative = downward. Empty fields = no data. Insignificant data (<6 standard deviations of field blank concentrations) given  
 183 as upper limits.

184 a.

	ACE	PHE	FLT	PYR
3 July D		-28.46	1.80	0.59
3-4 July N				
4 July D		-2.41	0.94	1.56
4-5 July N				
5 July D		-1.33	0.97	0.33
5-6 July N				
6 July D	-0.34	-4.84	< $\pm 0.25$	< $\pm 0.24$
6-7 July N				
7 July D	0.16	< $\pm 2.26$	< $\pm 0.47$	< $\pm 0.46$
7-8 July N				
8 July D	0.12	-4.72	-2.57	-1.02
8-9 July N				
9 July D				
9-10 July N				
10 July D		-2.06	-2.97	-1.32
10-11 July N				
11 July D				
11-12 July N		< $\pm 1.44$	-0.59	< $\pm 0.29$
12 July D		< $\pm 1.57$	-0.51	< $\pm 0.32$
12-13 July N		< $\pm 1.03$	< $\pm 0.21$	< $\pm 0.21$
13 July D		< $\pm 0.89$	-1.06	-0.44

185

b.

	$\alpha$ -HCH	$\gamma$ -HCH	PCB28	PCB52	PCB101	<i>p,p'</i> -DDE	PBDE47	PBDE99
3 July D	-2.61	-3.45	-0.60	-0.47	-0.17	< $\pm$ 0.03		
3-4 July N								
4 July D	-0.69	-1.79	-0.30	-0.19	-0.06	< $\pm$ 0.03		
4-5 July N								
5 July D	-0.37	-0.78	-0.15	-0.09	-0.03	< $\pm$ 0.02		
5-6 July N								
6 July D	-0.26	-0.62	-0.09	-0.04			0.91	< $\pm$ 1.09
6-7 July N								
7 July D	< $\pm$ 0.12	0.25	< $\pm$ 0.10	< $\pm$ 0.04				
7-8 July N								
8 July D	< $\pm$ 0.12	0.11	< $\pm$ 0.10	< $\pm$ 0.04			< $\pm$ 1.47	< $\pm$ 2.08
8-9 July N								
9 July D	< $\pm$ 0.13	0.23	< $\pm$ 0.10	< $\pm$ 0.04				
9-10 July N								
10 July D	< $\pm$ 0.08	-0.21	< $\pm$ 0.06	< $\pm$ 0.03	< $\pm$ 0.03	0.04		
10-11 July N								
11 July D	< $\pm$ 0.06	0.26	< $\pm$ 0.05	< $\pm$ 0.02		< $\pm$ 0.02		
11-12 July N		-0.12	< $\pm$ 0.06	< $\pm$ 0.03				
12 July D		< $\pm$ 0.08	< $\pm$ 0.07	< $\pm$ 0.03				
12-13 July N		< $\pm$ 0.05	< $\pm$ 0.04	< $\pm$ 0.02				
13 July D	< $\pm$ 0.05	0.18	-0.04	< $\pm$ 0.02		< $\pm$ 0.02		

186

187

## 1 S2.4 Seawater concentration data

2 Table S6. Concentrations in surface seawater at two localities west of Selles Beach and  
3 arithmetic mean ( $\text{pg L}^{-1}$ ).

	$c_w$ at locality 1	$c_w$ at locality 2	mean $c_w$
FLT	21.2	15.3	18.2
PYR	6.3	2.6	4.4
PCB 28	4.73	4.58	4.65
PCB 52	0.53	0.54	0.54
PCB 101	0.84	0.85	0.84
<i>p,p'</i> -DDE	0.75	0.93	0.84
BDE 47	0.12	0.18	0.15
BDE 99	0.039	0.037	0.038

4

## 5 S2.5 Model predicted concentrations and air-sea exchange flux

6 During the period 6–10 July, Crete was under influence of a constant northerly flow during day  
7 and night without change of air mass (see above, S2.1).

8 Many pollutants showed pronounced night-time maxima:  $c_{\text{day}}/c_{\text{night}} = 0.3\text{--}0.5$  for HCH isomers,  
9  $0.6\text{--}0.7$  for ACE, PHE, DDE and PCB52. For other species this was less pronounced or no  
10 day/night trend was observed ( $c_{\text{day}}/c_{\text{night}} = 0.8\text{--}0.9$  for PCB28, FLT, PYR,  $1.1\text{--}1.3$  for PBDEs)  
11 (Fig. 1).

12 During on-shore advection many contaminants' concentrations were influenced by BL depth, as  
13 indicated by anti-correlation with PAHs and OCPs (except DDE;  $r = -0.76 - -0.37$  i.e.,  
14 significant for  $\alpha$ -HCH on the  $p < 0.05$  confidence level, t-test). BL depth was not correlated with  
15 PCBs' and DDE concentrations ( $|r| < 0.45$ ). These findings indicate sea surface sources.

16 Using the 2-box fugacity model (above, S1.4), air-sea mass exchange fluxes,  $F_{\text{em}}$ , in the range -  
17  $1000 - +10 \text{ ng m}^{-2} \text{ h}^{-1}$  (positive defined upward) and atmospheric concentrations fed by  $F_{\text{em}}$  only  
18 in the range  $0.01\text{--}2.2 \text{ ng m}^{-3}$  are simulated (Table S6).

19

20 Table S6. Predicted concentrations in the marine atmospheric BL and surface seawater (mean  
 21 (min-max),  $\text{ng m}^{-3}$ ) and air-sea mass exchange fluxes,  $F_{em}$  (mean (min-max),  $\text{ng m}^{-2} \text{h}^{-1}$ )

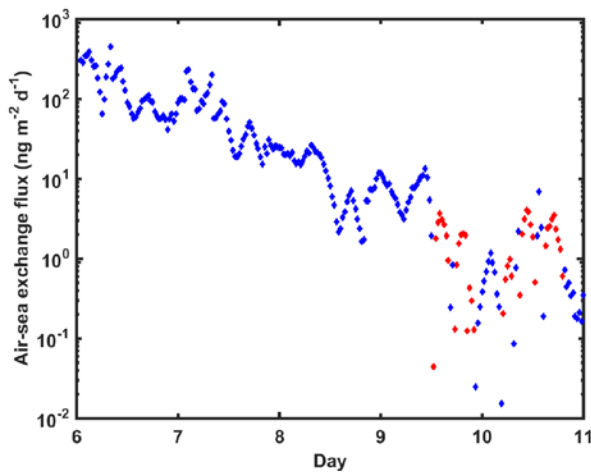
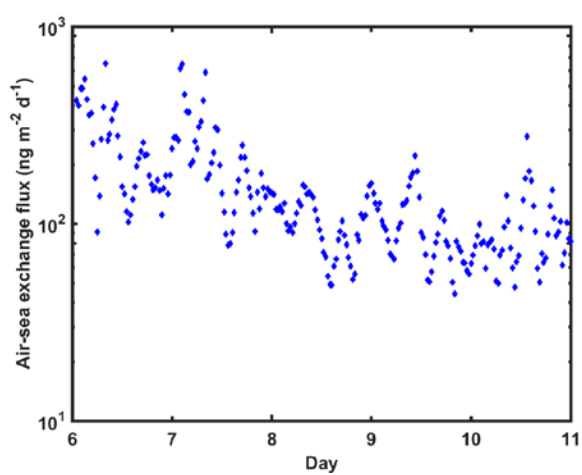
	$c_a$ ( $\text{ng m}^{-3}$ )	$c_w$ ( $\text{ng m}^{-3}$ )	$F_{em}$ ( $\text{ng m}^{-2} \text{d}^{-1}$ )
FLT	0.51 (0.13–2.27)	20.6 (18.2–22.0)	-3.20 (-13.6–0.00)
PYR	0.13 (0.01–1.13)	5.41 (4.44–5.60)	-0.96 (-9.32–0.08)
PCB28	0.037 (0.011–0.11)	4.60 (4.55–4.65)	0.061 (-0.009–0.14)
PCB52	0.016 (0.005–0.049)	0.54 (0.54–0.54)	-0.007 (-0.041–0.007)
BDE47	0.45 (0.12–2.04)	4.00 (0.15–6.41)	-5.22 (-20.0–0.00)
BDE99	0.25 (0.051–1.27)	3.34 (0.49–4.89)	-3.69 (-15.3–0.00)

22

23 Fig. S4. Predicted vertical flux,  $F_c$  (red upward and blue downward,  $\text{ng m}^{-2} \text{d}^{-1}$ ), of (a) FLT, (b)  
 24 PYR, (c) PCB28, (d) PCB52, (e) PBDE47 and (f) BDE99 during 6-10 July 2012.

25 a.

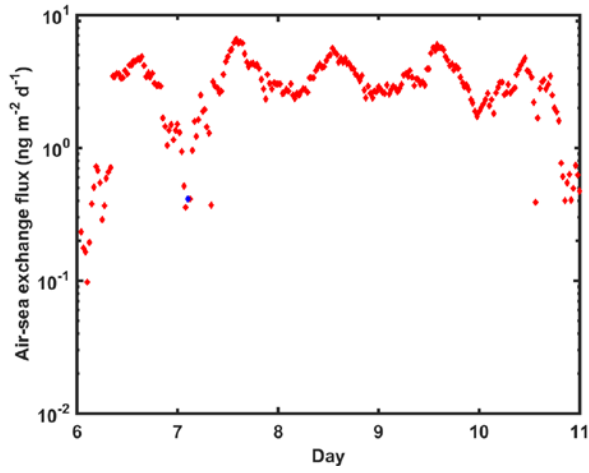
b.



26

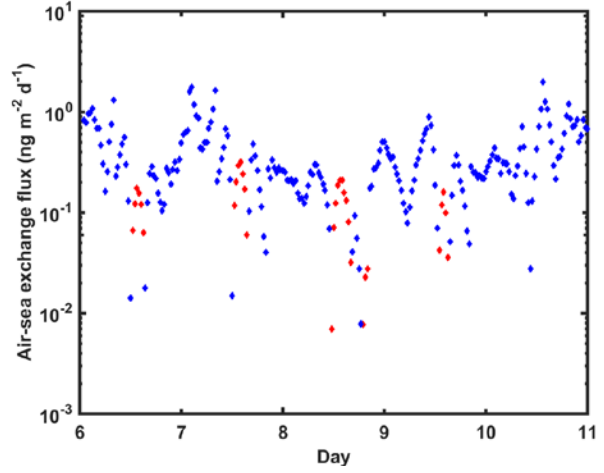
27 c.

d.

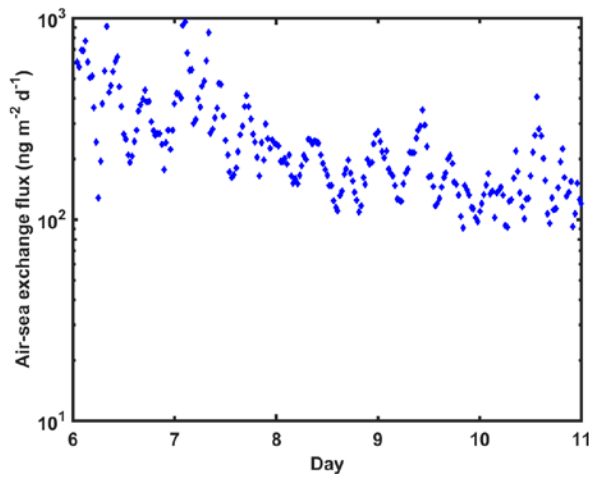


28

29 e.

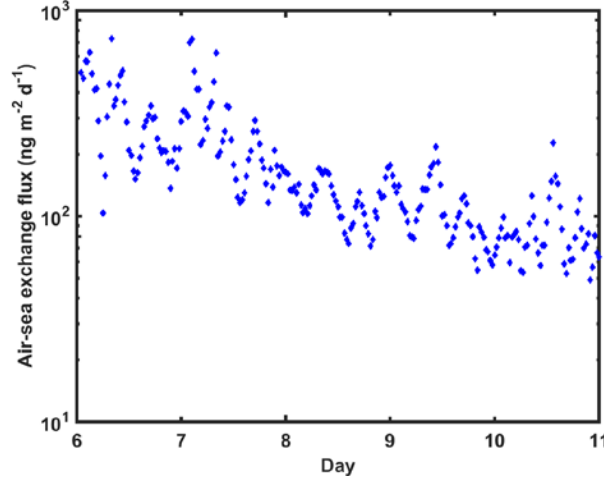


f.



30

31



## 32 References

- 33 Anderson, P.N., Hites, R.A., 1996. Hydroxyl radical reactions: The major pathway for polychlorinated  
34 biphenyls from the atmosphere. *Environ. Sci. Technol.* 30, 1756-1763.
- 35 Bamford, H.A., Poster, D.L., Baker, J.E., 1999. Temperature dependence of Henry's law constants of  
36 thirteen polycyclic aromatic hydrocarbons between 4°C and 31°C, *Environ. Toxicol. Chem.* 18, 1905-  
37 1912.
- 38 Beyer, A., Mackay, D., Matthies, M., Wania, F., Webster, E., 2000. Assessing long-range transport  
39 potential of persistent organic pollutants, *Environ. Sci. Technol.* 34, 699-703.
- 40 Cetin, B., Odabasi, M., 2005. Measurement of Henry's law constants of seven polybrominated  
41 diphenylethers (PBDE) congeners as a function of temperature. *Atmos. Environ.* 39, 5273-5280
- 42 Cetin, B., Özer, S., Sofuoglu, A., Odabasi, M., 2006. Determination of Henry's law constants of  
43 organochlorine pesticides in deionized and saline water as a function of temperature. *Atmos. Environ.*  
44 40, 4538-4546.
- 45 d'Ortenzio, F., Iudicone, D., de Boyer Montegut, C., Testor, C., Antoine, D., Marullo, S., Santoleri, R.,  
46 Madec, G., 2005. Seasonal variability of the mixed layer depth in the Mediterranean Sea as derived  
47 from in situ profiles, *Geophys. Res. Lett.* 32, L12605.
- 48 Dyer AJ, 1974. A review of flux-profile relationships. *Boundary-Layer Meteor.* 7, 363-372
- 49 EU, 1996. Technical guidance document in support of the commissions directive 5 93/67/EEC on risk  
50 assessment for the notified substances and the commission regulation (EC) 1488/94 on risk  
51 assessment for existing substances.
- 52 Foken, T., 2008. *Micrometeorology*, Springer, Heidelberg, 308 pp.
- 53 Franklin, J., Atkinson, R., Howard, P.H., Orlando, J.J., Seigneur, C., Wallington, T.J., Zetzsch, C., 2000.  
54 Quantitative determination of persistence in air, in: *Evaluation of Persistence and Long-Range*  
55 *Transport of Organic Chemicals in the Environment* (Klecka, G.M., et al., eds.), SETAC Press,  
56 Pensacola, USA, pp. 7–62.
- 57 Hayward, S.J., Lei, Y.D., Wania, F., 2006. Comparative evaluation of three HPLC-based  $K_{ow}$  estimation  
58 methods for highly hydrophobic organic compounds: PBDEs and HBCD, *Environ. Toxicol. Chem.*  
59 25, 2018-2027.
- 60 Hicks, B.B., Baldocchi, D.D., Meyers, T.P., Hosker, R.P., Matt, D.R., 1987. A preliminary multiple  
61 resistance routine for deriving dry deposition velocities from measured quantities, *Water Air Soil*  
62 *Poll.* 36, 311–330.
- 63 Jantunen, L.M., Bidleman, T.F., 2006. Henry's law constants for hexachlorobenzene, *p,p'*-DDE and  
64 components of technical chlordane and estimates of gas-exchange for Lake Ontario, *Chemosphere* 62,  
65 1689-1696.
- 66 Jonker, M.T.O., Muijs, B., 2010. Using solid phase micro extraction to determine salting-out  
67 (Setschenow) constants for hydrophobic organic chemicals. *Chemosphere* 80, 223–227.
- 68 Karickhoff, S.W., 1981. Semi-empirical estimation of sorption of hydrophobic pollutants on natural  
69 sediments and soils. *Chemosphere* 10, 833-849.
- 70 Keyte, I.J., Harrison, R.M., Lammel, G., 2013. Chemical reactivity and long-range transport potential of  
71 polycyclic aromatic hydrocarbons – a review, *Chem. Soc. Rev.* 42, 9333-9391
- 72 Kuhn, U., Andreae, M.O., Ammann, C., Araujo, A. C., Brancaleoni, E., Ciccioli, P., Dindorf, T.,  
73 Frattoni, M., Gatti, L. V., Ganzeveld, L., Kruijft, B., Lelieveld, J., Lloyd, J., Meixner, F. X., Nobre, A.  
74 D., Pöschl, U., Spirig, C., Stefani, P., Thielmann, A., Valentini, R., Kesselmeier, J., 2007. Isoprene  
75 and monoterpene fluxes from Central Amazonian rainforest inferred from tower-based and airborne  
76 measurements, and implications on the atmospheric chemistry and the local carbon budget, *Atmos.*  
77 *Chem. Phys.* 7, 2855–2879.

78 Li, N., Wania, F., Lei, Y.D., Daly, G.L., 2003. A comprehensive and critical compilation, evaluation, and  
79 selection of physical-chemical property data for selected polychlorinated biphenyls. *J. Phys. Chem.*  
80 *Ref. Data*, 32, 1545–1590.

81 Lohmann, R., Klánová, J., Kukučka, P., Yonis, S., Bollinger, K., 2012. PCBs and OCPs on a east to west  
82 transect: The importance of major currents and net volatilization for PCBs in the Atlantic Ocean,  
83 *Environ. Sci. Technol.* 46, 10471-10479.

84 Monin, A.S., Obukhov, A.M., 1954. Osnovnye zakonmernosti turbulentnogo peremesivaniya v  
85 prizemnom sloe atmosfery, *Trudy geofiz. inst. AN SSSR*, 24(151), 163–187.

86 Mulder, M.D., Heil, A., Kukučka, P., Klánová, J., Kuta, J., Prokeš, R., Sprovieri, F., Lammel, G., 2014.  
87 Air-sea exchange and gas-particle partitioning of polycyclic aromatic hydrocarbons in the  
88 Mediterranean. *Atmos. Chem. Phys.* 14, 8905–8915.

89 Obukhov, A.M., 1948. Turbulentnost' v temperaturnoj - neodnorodnoj atmosfere, *Trudy geofiz. inst. AN*  
90 *SSSR* 1.

91 Paulson, C.A., 1970. The mathematical representation of wind speed and temperature profiles in the  
92 unstable atmospheric surface layer. *J. Appl. Meteor.* 9, 857-861.

93 Pujó-Pay, M., Conan, P., Oriol, L., Cornet-Barthaux, V., Falco, C., Ghiglione, J.F., Goyet, C., Moutin, T.,  
94 Prieur, L., 2011. Integrated survey of elemental stoichiometry (C, N, P) from the western to eastern  
95 Mediterranean Sea, *Biogeosci.* 8, 883-899.

96 Raff, J.D., Hites, R.A., 2007. Deposition vs. photochemical removal of PBDEs from Lake Superior air,  
97 *Environ. Sci. Technol.* 41, 6725-6731.

98 Rowe, A. A., Totten, L. A., Xie, M., Fikslin, T. J., Eisenreich, S. J., 2007. Air-water exchange of  
99 polychlorinated biphenyls in the Delaware river. *Environ. Sci. Technol.* 41, 1152–1158.

100 Schwarzenbach, R.P., Gschwend, P.M., Imboden, D.M., 2003: *Environmental Organic Chemistry*, 2<sup>nd</sup> ed.,  
101 Wiley, Hoboken, USA.

102 Spivakovsky, C.M., Logan, J.A., Montzka, S.A., Balkanski, Y.J., Foreman-Fowler, M., Jones, D.B.A.,  
103 Horowitz, L.W., Fusco, A.C., Brenninkmeijer, C.A.M., Prather, M.J., Wofsy, S.C., McElroy, M.B.,  
104 2000. Three-dimensional climatological distribution of tropospheric OH: update and evaluation. *J.*  
105 *Geophys. Res.* 105, 8931–8980.

106 Tittlemier, S.A., Halldorson, T., Stern, G.A., Tomy, G., 2002. Vapor pressures, aqueous solubilities, and  
107 Henry law constants of some brominated flame retardants. *Environ. Toxicol. Chem.* 21, 1804-1810.

108 USEPA, 2009. EPI Suite v4.0, Exposure assessment tools and models, US Environmental Protection  
109 Agency. <http://www.epa.gov/opt/exposure/pubs/episuitedl>.

110 Valavanis, V.D., Georgakarakos, S., Kapantagakis, A., Palialaxis, A., Katara, I., 2004. A GIS  
111 environmental modelling approach to essential fish habitat designation. *Ecol. Model.* 178, 417-427.

112 Wania, F., Daly, G., 2002. Estimating the contribution of degradation in air and deposition to the deep  
113 sea to the global loss of PCBs. *Atmos. Environ.* 36, 5581-5593.

114 Zhong G., Xie Z., Möller A., Halsall C., Caba A., Sturm R., Tang J., Zhang G., Ebinghaus R., 2012.  
115 Currently used pesticides, hexachlorobenzene and hexachlorocyclohexanes in the air and seawater of the  
116 German Bight (No